Electronic supplementary materials *Mendeleev Commun.*, 2024, **34**, 725–728

Pt/C electrocatalysts based on N-doped carbon materials from waste plant biomass

Daria V. Chernysheva, Victor A. Klushin, Anastasia A. Alekseenko, Elizaveta A. Moguchikh, Evgeny A. Kolesnikov, Mikhail V. Gorshenkov, Vasily V. Kaichev, Lev N. Fesenko and Nina V. Smirnova

EXPERIMENTAL

Synthesis

Synthesis of Pt/C electrocatalysts based on the obtained N-doped (NH-CK) and non-doped (H-CK) carbon materials from liquid humins was carried out by the liquid-phase method using formaldehyde as a reducing agent [S1]. For each synthesis, 0.15 g of carbon material and 20 mL of ethylene glycol were placed in a beaker and stirred on a magnetic stirrer for 30 min. Next, the suspension was homogenized by ultrasound. Aqueous solution of $H_2PtCl_6 \cdot 6H_2O$, aqueous solution of 1 M NaOH and 1 mL of formaldehyde (37.4%) were added to the suspension under constant stirring. Then, the reaction mixture was heated to 80 °C and kept at this temperature and constant stirring for 2 h. After completion of the synthesis, the heating was turned off and the suspension was cooled to room temperature for 1 h. Afterwards, an aqueous solution of 1 M sulfuric acid was added. The obtained catalysts were designated as Pt/NH-CK and Pt/H-CK, respectively.

Charecterization

The chemical composition of the carbon material NH-CK was studied by X-ray photoelectron spectroscopy (XPS). XPS measurements were performed on an X-ray photoelectron spectrometer equipped with a PHOIBOS-150-MCD-9 hemispherical analyzer and an XR-50 X-ray radiation source (SPECS Surface Nano Analysis GmbH, Germany). The core-level spectra were recorded using Al Kα radiation (hυ=1486.6 eV). The charge correction was performed by setting the most intense C*1s* peak at 284.8 eV. The relative concentrations of elements in the analysis zone are determined on the basis of the integral intensities of the XPS peaks, taking into account the photoionization cross section [S2]. For detailed analysis, the decomposition of spectra into individual components is used. Accordingly, after subtracting the background by the Shirley method, the experimental curve was decomposed into a number of peaks corresponding to the photoemission of electrons from atoms in different chemical environments. Data processing was performed using the CasaXPS software. The peak shape is approximated by the symmetric function obtained by summing the Gauss and Lorentz functions.

Electrochemical measurements

Cyclic voltammetry (CV) was provided in a three-electrode cell filled with 0.1 M $HClO_4$ solution saturated with Ar at atmospheric pressure and 25 °C. The reference electrode is a saturated silver chloride electrode, the counter electrode is Pt wire. All potentials are given relative to the reversible hydrogen electrode (RHE). The working electrode was a catalytic layer based on catalytic "ink" formed on a glass-graphite disk electrode. For the preparation of catalytic "ink", the mass of the sample was calculated so that when the catalyst was subsequently applied to the electrode, the mass of platinum was 20-32 $\mu g(Pt)/cm^2$. Then 1% aqueous emulsion of Nafion® polymer, deionized water and isopropyl alcohol was added. A detailed description of the methodology of "ink" preparation is presented in Ref. [S3]. Before immersing the working electrode into the electrolyte solution, its surface was wetted with 0.1 M perchloric acid. The measurements were performed using a Pine Research MSR Rotator (USA).

Surface standardization was performed in the potential range of 0.04-1.0 V at a potential sweep rate of 100 mV/s. The electrochemically active surface area (ESA) was calculated by the formula:

$$\mathrm{ESA} = (Q_{ad} + Q_d)/(R \cdot m \cdot 1000),$$

were Q_{ad} (Q_d) is amount of electricity consumed for adsorption (desorption) of hydrogen in the hydrogen region in the potential range of 0.04-0.35 V on CV curve taken at a potential sweep rate of 20 mV/s in the potential range of 0.04-1.0 V;
R is amount of electricity consumed for adsorption/desorption of hydrogen monolayer (210 μC/cm^2);
m is mass of Pt on the electrode.
The allowable error is ± 10%.

To evaluate the activity of the catalysts in the oxygen reduction reaction, the background potentiodynamic polarization curve was measured in an argon-saturated electrolyte at a disk electrode rotation speed of 1600 rpm in the potential range of 0.1-1.1 V with a potential sweep rate of 20 mV/s. Then the electrolyte in the cell was saturated with oxygen for one hour, after which potentiodynamic curves were measured at a potential sweep rate of 20 mV/s in the potential range from 0.1 to 1.1 V at four rotational speeds of the disk electrode: 400, 900, 1600, and 2500 rpm. The potential was recalculated to the RHE taking into account the resistance (iR-compensation) and the potential of the reference electrode according to the formula:

$$E_{RHE} = E + E_{RE} + E_{pH} - iR,$$

where E is set potential value, V
E_{RE} is potential value of the reference electrode, V
E_{pH} is pH correction of the solution equal to 0.059 V at 25 °C, V
iR is ohmic potential drop equal to the product of the current strength and the resistance of the solution layer between the reference electrode and the working electrode.

The contribution of processes occurring at the electrode in deoxygenated solution (Ar atmosphere) was taken into account by subtracting from the voltammetry currents the currents of the background curve measured in Ar atmosphere at each potential value according to the formula:

$$I_p = I_{(O2)} - I_{(Ar)}.$$

The calculation of the kinetic current density (j_k) at a potential of 0.50 V was performed using the Koutecký–Levich equation [S1, S4]:

$$1/j = 1/j_k + 1/j_d,$$

where j is the experimentally measured current, j_d is the diffusion-limited current, and j_k is the mass-transport free kinetic current. The kinetic currents were calculated for a potential of 0.5 V (RHE). The number of electrons involved in ORR was determined by the slope of the line in coordinates j^{-1} - $\omega^{-0.5}$. The allowable error is ± 20%.

The stability of the catalysts was assessed by stress testing method based on multiple voltammetric cyclic potential changes at a rate of 100 mV/s for 3000 cycles in the potential range of 0.6–1.0 V (RHE) [S5]. Measurements were carried out in an air-saturated 0.1 M $HClO_4$ solution at 25 °C. At the beginning of stress test and after every 500 cycles, two CVs were recorded in the potential range of 0.04–1 V (RHE) at a potential sweep rate of 20 mV/s. The ESA was calculated using the second CV as described above. Stability was assessed by the change in ESA of the catalysts during the stress test (ESA_{0-3000}) relative to the ESA measured before starting the stress test (ESA_0) (Figure S1).

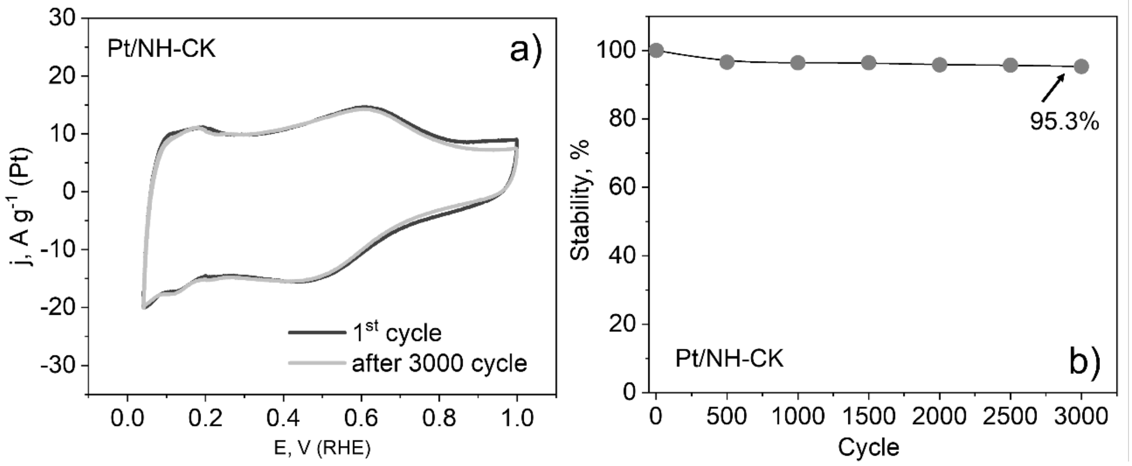

Figure S1. The stability of the Pt/NH-CK catalyst: a) CV curves before and after multiple voltammetric cyclic potential changes at a rate of 100 mV/s for 3000 cycles in the potential range of 0.6–1.0 V; b) stability of the catalyst during stress testing.

The oxygen reduction reaction pathways (* denotes the active site of the catalyst) [S6]:

Four-electron pathway:

$O_2 + 4H^+ + 4e^- \rightarrow {}^*OOH + 3H^+ + 3e^- \rightarrow {}^*O + 2H^+ + 2e^- \rightarrow {}^*OH + H^+ + e^- \rightarrow 2H_2O$

Two-electron pathway:

$O_2 + 2H^+ + 2e^- \rightarrow {}^*OOH + H^+ + e^- \rightarrow H_2O_2$

The mechanism of nitrogen doping

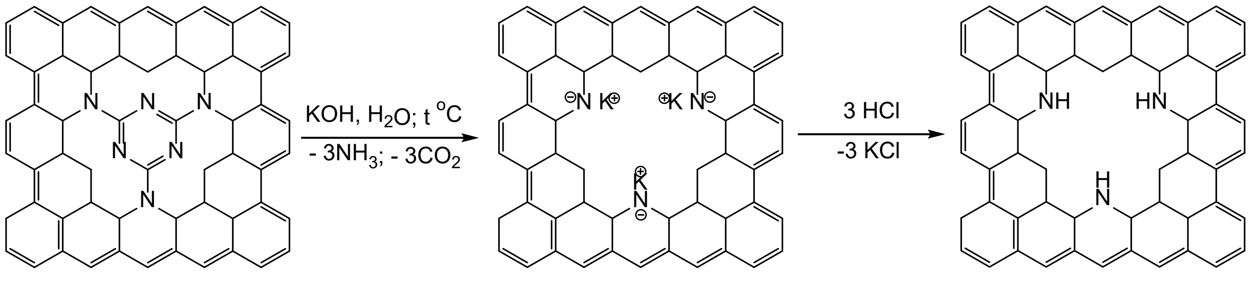

Scheme S1 Assumed scheme of nitrogen incorporation into the carbon framework in pyridinic N configuration during the process of thermochemical conversion of initial NH polymer [S7].

REFERENCES

S1 K. O. Paperzh, A. A. Alekseenko, V. A. Volochaev, I. V. Pankov, O. A. Safronenko and V. E. Guterman, *Beilstein J. Nanotechnol.,* 2021, **12**, 593; https://doi.org/10.3762/bjnano.12.49.

S2 J. H. Scofield, *J. Electron Spectrosc. Relat. Phenom.,* 1976, **8**, 129; https://doi.org/10.1016/0368-2048(76)80015-1.

S3 K. Paperzh, A. Alekseenko, O. Safronenko, A. Nikulin, I. Pankov and V. Guterman, *Colloid Interface Sci. Commun.,* 2021, **45**, 100517; https://doi.org/10.1016/j.colcom.2021.100517.

S4 K. Shinozaki, J. W. Zack, R. M. Richards, B. S. Pivovar and S. S. Kocha, *J. Electrochem. Soc.,* 2015, **162**, F1144; https://doi.org/10.1149/2.1071509jes.

S5 E. A. Moguchikh, K. O. Paperzh, A. A. Alekseenko, E. N. Gribov, N. Y. Tabachkova, N. V. Maltseva, A. G. Tkachev, E. A. Neskoromnaya, A. V. Melezhik, V. V. Butova, O. I. Safronenko and V. E. Guterman, *J. Appl. Electrochem.,* 2022, **52**, 231; https://doi.org/10.1007/s10800-021-129-y.

S6 X. Hu, B. Yang, S. Ke, Y. Liu, M. Fang, Z. Huang and X. Min, *Energy Fuels,* 2023, **37**, 11532; https://doi.org/10.1021/acs.energyfuels.3c01265.

S7 D. V. Chernysheva, E. A. Sidash, M. S. Konstantinov, V. A. Klushin, D. V. Tokarev, V. E. Andreeva, E. A. Kolesnikov, V. V. Kaichev, N. V. Smirnova and V. P. Ananikov, *ChemSusChem,* 2023, **16**, e20220206; https://doi.org/10.1002/cssc.202202065.